Oxid Met (2009) 71:257–270
DOI 10.1007/s11085-009-9141-6

ORIGINAL PAPER

Oxidation Resistance of Cast Magnesium Alloys

Jožef Medved · Primož Mrvar · Maja Vončina

Received: 3 October 2008 / Revised: 5 January 2009 / Published online: 19 March 2009

Abstract The purpose of the present study was to examine the oxidation of Mg–Al alloys in the atmosphere of oxygen at various temperatures. The basic examination methods used were differential scanning calorimetry (DSC) and thermogravimetry (TG). The results show that the oxide layer can either protect the material against progressive oxidation or it can cause complete disintegration of material. The nature of the oxide layer formed depends on the external conditions, i.e. on the atmosphere, temperature, and type of alloy. A model of the Mg–Al alloy oxidation was calculated from the TG curves.

Keywords Mg-alloys · Oxidation · Thermodynamics · DSC · TG

Introduction

Because of the rapid development in automotive, aircraft and power industries, the use of light alloys and their development has extensively increased. This increase is especially evident in the use of light magnesium alloys. The advantage of the Mg-alloys is in the mass/strength ratio, i.e. small mass of final products and their good mechanical properties; these alloys also have a good corrosion resistance [1].

Magnesium alloys are usually used at room temperatures but they can also stay at higher temperatures and oxidizing atmospheres in different stages of processing, such as: overheating of the charge, melting, casting, heat treatment and mechanical processing, recycling etc. But those conditions result undesirable effects that change

J. Medved · P. Mrvar · M. Vončina (✉)
Department of Materials and Metallurgy, Faculty of Natural Sciences and Engineering, University of Ljubljana, Aškerčeva 12, 1000 Ljubljana, Slovenia
e-mail: maja.voncina@ntf.uni-lj.si

chemical properties and deteriorate structural properties of the surface layers. Therefore the knowledge of oxidation of Mg-alloys at different temperatures is important for development of new Mg-based materials and the optimization of their technological processes.

Various Mg alloys: AE42, AZ91, AM50, and AM60 were exposed to oxidation at different temperatures in order to determinate high-temperature oxidation resistance.

Oxidation of Magnesium

Low Temperature Oxidation

Corrosion of all grades of magnesium and Mg-alloys is of the electrochemical nature [2]. High corrosion potential is needed due to the high negative standard electrode potential of Mg. In pure or alkaline water $Mg(OH)_2$ passive films of crystalline nature are formed on the surface of magnesium [3]. In the water solution having pH <10 this passive layer is unstable because of high compressive stresses inside the layer (geometric incompatibility with the Mg-lattice), causing the separation of layer and the commencement of corrosion. Hydrogen liberated in corrosion causes further separation of this passive layer. In pure alkaline water solution with pH >10.5 the layer is very stable. In water solutions containing chloride, sulphide, or carbonate ions (fluoride ions are exception), the passive $Mg(OH)_2$ layer is destroyed and dissolved. Such corrosion occurs if magnesium is exposed to exhaust gases, acid rain, and salts.

In the same way corrosion attacks the whole passive layer. The corrosion of Mg has two magnitudes. Higher values of corrosion are obtained in the solutions containing chloride or sulphide ions than in pure distilled water. Formation of hydrogen is the main cathode reaction in this corrosion mechanism. The source of porous corrosion layer is in the inhomogeneous crystal structures, e.g., when $Mg_{17}Al_{12}$ phase is precipitated on grain boundaries. These structures have higher standard potential and they cause electrolytic process within the surrounding matrix. This electrochemical corrosion creates traces of porous corrosion product [3, 4]. In the Mg alloys, the pressure corrosion cracking appears when the internal or external tensile stresses are combined with the effect of corrosion media (chloride, sulphide and chlorate solutions). This leads to brittleness at the crack points because hydrogen, formed during the corrosion process, is absorbed [3].

Electrochemical corrosion appears because of formation of galvanic cells. It frequently occurs in the Mg alloys that contain more electrochemically stable metals (alloy components or impurities), e.g., heavy metals, especially iron, copper, and nickel that are in electric contact with the matrix. Electrochemical corrosion is intensified in the high-purity Mg-alloys and in dry atmosphere (when no electrolyte is present).

Corrosion resistance of Mg-alloys [3] is increased with higher purity of alloys, with addition of special alloying elements (Y, Nd, La, Zr and Ce), and with surface treatment procedures (cleaning of surface, colouring, anodic treatment…).

High-temperature Oxidation

The course of high-temperature oxidation of magnesium is linear. At higher temperatures, particularly around 437 °C (eutectic temperature) [5], a different behaviour was noticed at Mg–Al alloys. The obvious difference at higher temperatures resulted from the fact that chemical properties and relative volumes of phases in Mg–Al alloys were changed because of the diffusion process. The alloys at lower temperatures form transformed eutectic; but at temperatures above 437 °C the eutectic spheroidizes and progressively decays, while the magnesium region is homogenized throughout the matrix. Aluminium, that is the main alloying element, has a very different oxidizing and volatilization properties from Mg. Though aluminium itself forms a very resistant film of Al_2O_3, the addition of over 1 mass% Al increases the oxidation of magnesium [6].

It is known that in the atmosphere containing oxygen, the growth of oxide film is diffusion controlled in the solid state, forming a compact oxide surface. In Mg-alloys at higher temperatures the lattice diffusion is reduced due to a noticeable lack of simple ways for quick transport of Mg vapours to the surface. Therefore the oxide film stays stable and protective for a longer time. Diffusivity of Mg in MgO lattice is known, and it is [7]: $D = 1.0 \cdot 10 \exp(-150/RT)\ m^2/s$.

Observations show that the thin oxide layer that is formed presents a good protection [6]. At lower temperatures transformed eutectic is formed in the alloy. It spheroidizes and progressively decays at temperatures above 437 °C, while, as already mentioned, the magnesium region is homogenized throughout the matrix. Protective oxide film is destroyed by formation of the so-called oxide spongy spots (Fig. 1) [8]. The morphology of the oxide spongy spots that are randomly distributed on the surface of the alloy does not show any evident uniform growth of those spots. Such type of structures shows the formation of "fresh" oxide on oxide/metal contacts and on the surfaces. It is believed that these spongy spots are formed in the presence of the oxygen penetrating through the cracks. This creates the condition for the reaction between oxygen and metal on crack walls and a spongy oxide layer is formed. The intensity of this reaction depends on the size of cracks

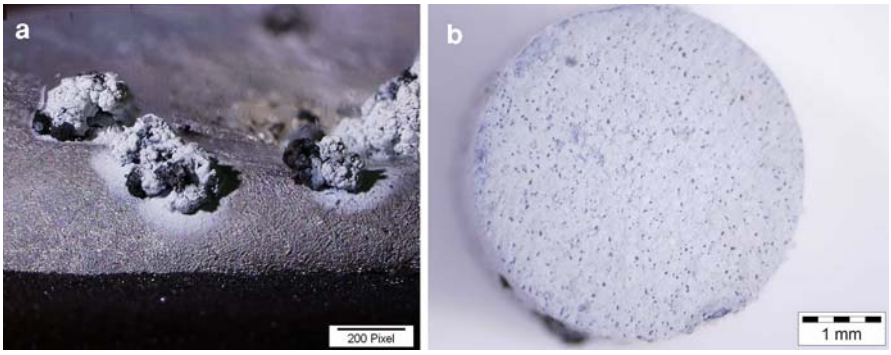

Fig. 1 Morphology of protective oxidation and growth of the oxide sponges [8]. **a** Protective oxide layer. **b** The growth of oxide sponges

and the rate of their healing, respectively, filling the cracks with fresh oxygen. The growth of thick MgO layers is controlled by the first-order reaction. Generally, it is desirable that such a type of uncontrolled oxidation does not depend on the thickness of layer. It is also confirmed that oxygen can easily penetrate through the surface of the metal.

The correlation between the thermo-gravimetric kinetics and the microstructure demonstrates that there is a relation between the increasing oxidation and the growth of oxide sponges. The growth of these sponges is activated in the stage of inhomogeneity, especially during the formation of the metal liquid phase with high vapour pressure of magnesium. At high temperatures magnesium can sublimate by the diffusion through the oxide film after the incubation period. Of greater importance is the elimination of Mg vapours from the metal surface. They cause that compact oxide film decays into a porous layer. Above 437 °C the degree of Mg volatility is so high that vapour does not only fill up all the pores in nodules but also fills the surface where the oxide films are formed. The opened oxide sponges continue to grow by the transfer of magnesium vapours through the pores and simultaneous reaction with the oxygen forming a product that has morphology of "a cauliflower". It was noticed that the simultaneous oxidation of magnesium led to formation of an alloy, where oxide fills up the places of the "consumed" metal. It seems that oxidation is intensified with time and at temperatures higher than 472 °C and it is also related to the enlargement of spots and pores. [9, 10] These spots and pores are suitable for vapour condensing inside the layer, and this increases the surface of metal that is exposed to oxygen. Further growth of the oxide film depends on the selection of oxidizing components of the alloy that stimulate the reaction on the surface between the oxide and metal, and this increases the surface available for evaporation.

The progress of oxidation was experimentally determined with the TG curves for the Mg–Al alloys. A physical model was calculated on the basis of this time relationship. A model of the Mg–Al alloy oxidation [8] was calculated from the TG curves, as:

$$\Delta m = 5E - 0.5t^3 - 0.0022t^2 - 0.0315t + 100.01\ [\%] \text{ protective oxidation}$$
$$\Delta m = 0.159t^4 - 2.0942t^3 + 103.72t^2 - 2277.8t + 118597\ [\%] \text{ progressive oxidation}$$

Experimental Work

Cylindrical samples with 4.0 mm diameter and 2.0 mm height were prepared and placed on platinum carrier (Fig. 2). The samples were examined thermogravimetrically (TG) with the 449c Jupiter Instrument (NETZSCH) for simultaneous thermal analysis (STA). They were heated in protective atmosphere (nitrogen) to various oxidation temperatures (200, 400, 450 and 500 °C), with the heating rate of 10 K/min. The samples were then held in oxygen atmosphere for 12 h and afterwards cooled at 10 K/min to the room temperature. After the DSC analysis the macrographs of specimens were made with the Olympus SZ61 stereomicroscope.

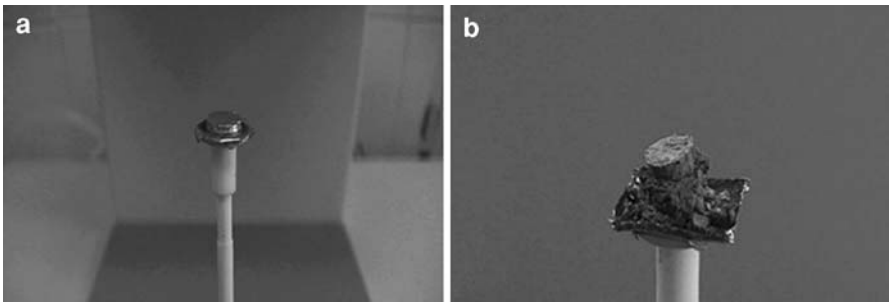

Fig. 2 Sample on the TG carrier made of platinum. **a** Before the experiment. **b** After the experiment

Table 1 The chemical composition of examined alloys

Alloy	Mg (mass%)	Al (mass%)	Si (mass%)	Mn (mass%)	Zn (mass%)	RE (mass%)
AE42	Rest	4.2	0.03	0.29	0.15	1.5
AM50	94.7	4.7	–	0.40	0.12	–
AM60	93.7	5.84	0.028	0.33	0.05	–
AZ91	Rest	8.5–9.5	–	0.17–0.4	0.45–0.9	–

Chemical composition of the examined alloys is presented in Table 1.

DSC analyses were made with all the alloy samples. Atomic force microscopy (AFM) was used to determine the shape of oxides in the specimen from AM60 oxidized at 400 °C.

Results and Discussion

In Figs. 3, 4, 5, 6 the TG curves of oxidation and the macrographs of examined alloys are presented. At low oxidation temperature (200 °C) a thin oxide layer was formed on the sample surface. In oxidation of AM50, AM60, and AE42 alloys a small increase of mass in the range of 0.1–0.5 mass% was found; in the AZ91 alloy the mass was reduced for approximately 0.1 mass%.

At 400 °C the oxidation of the AE42 alloy was quite scarce and a change of mass of approximately 0.1 mass% was determined; in the AZ91alloy the change of mass was higher, 0.85 mass%. At the temperature of 450 °C, an excessive oxidation of the AZ91 alloy took place as also reported by [9, 10]. In the oxidation of the AM50, AM60, and AE42 alloys the change of mass was higher and it varied between 0.2 and 3.8 mass%. At the highest oxidation temperature (500 °C), the change of mass in the AE42 alloy was 0.7 mass%. At the oxidation temperature of 500 °C the highest mass change was found for the AM60 alloy, it exceeded 30 mass%.

The specimen taken from the AM60 alloy before and after the 12 h oxidation at the temperature of 400 °C was analysed by the AFM analysis too (Fig. 7).

Figure 7a gives evidence only of abrasion on the specimen surface. Here the oxidation did not take place. Figure 7b presents the surface of the specimen after the

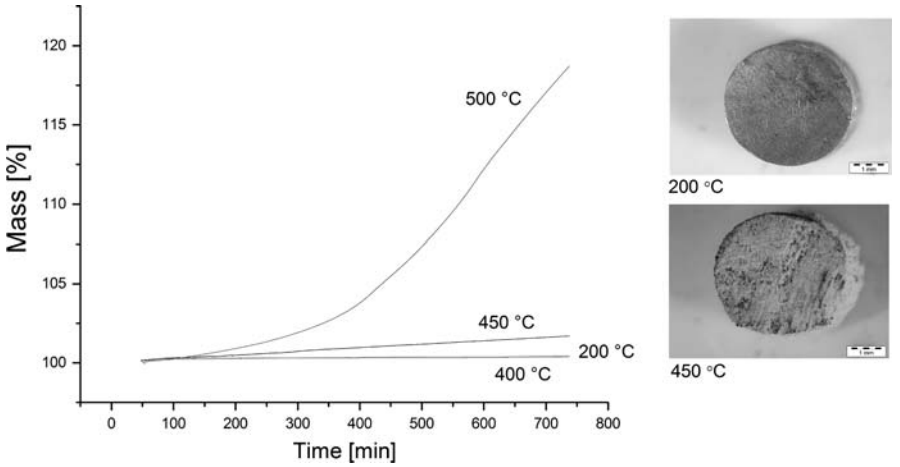

Fig. 3 TG curves and macrographs of examined specimen of the AE42 alloy

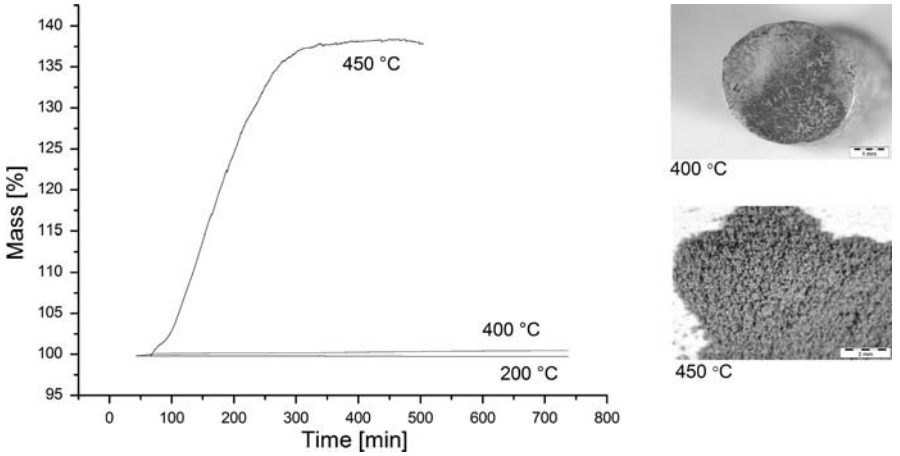

Fig. 4 TG curves and macrographs of examined specimen of the AZ91 alloy

oxidation at 400 °C for 12 h. On the surface oxide sponges that were formed in the oxidation atmosphere were evident.

The comparison of various alloys at the same temperature (Figs. 8, 9, 10, 11) showed that all the alloys had good corrosion resistances at low temperatures (200 °C and 400 °C). At higher temperatures the AZ91 alloy was unstable; the most stable alloy was the AE42 alloy. The corrosion stability was reduced with higher Al additions.

The kinetic models of examined alloys are described by the following equations (time t is in minutes):

At 200 °C:

$$\Delta m_{AM50} = 99.87651 + 8.17415 \times 10^{-4}t - 4.80721 \times 10^{-7}t^2$$

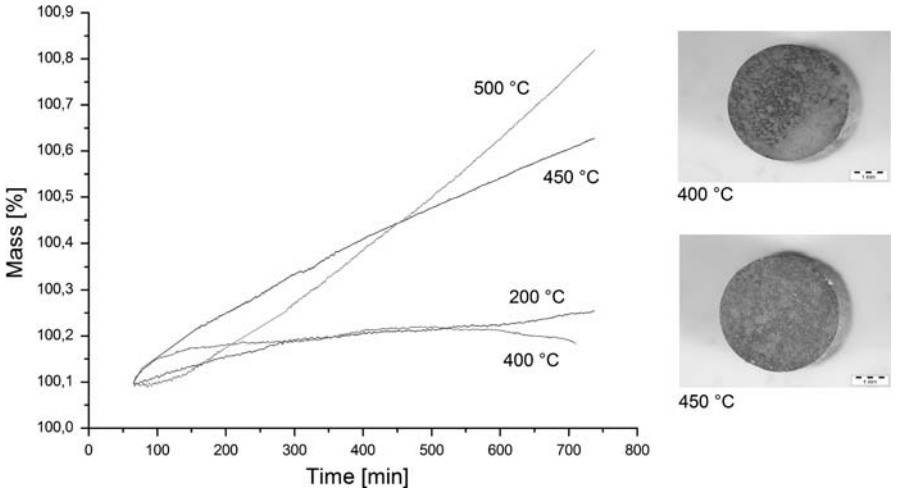

Fig. 5 TG curves and macrographs of examined specimen of the AM50 alloy

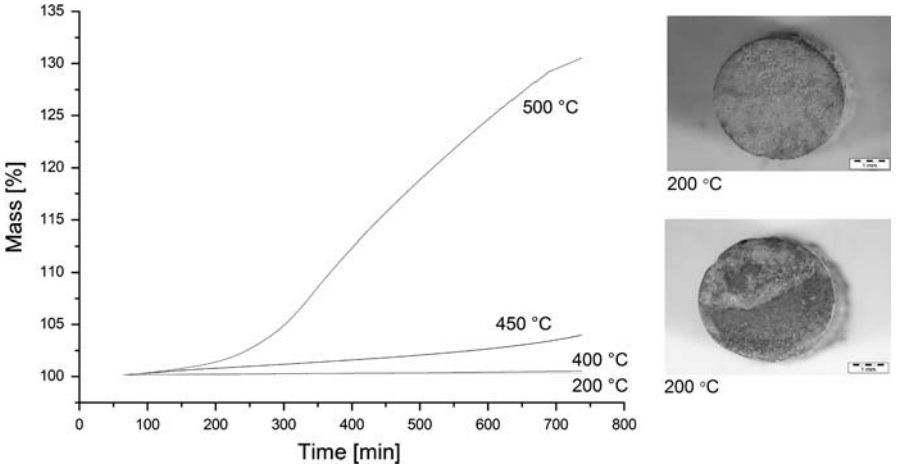

Fig. 6 TG curves and macrographs of examined specimen of the AM60 alloy

$$\Delta m_{AZ91} = 99.98293 - 0.00112t + 7.52251 \times 10^{-6}t^2 - 2.32339 \times 10^{-8}t^3 + 3.04034 \times 10^{-11}t^4 - 1.40687 \times 10^{-14}t^5$$

$$\Delta m_{AE42} = 99.87012 + 8.42615 \times 10^{-4}t - 1.47838 \times 10^{-6}t^2 + 9.88355 \times 10^{-10}t^3$$

$$\Delta m_{AM60} = 99.8961 + 4.16135 \times 10^{-4}t + 1.31073 \times 10^{-6}t^2 - 4.2518 \times 10^{-9}t^3 + 3.07167 \times 10^{-12}t^4$$

At 400 °C:

$$\Delta m_{AM50} = 99.97025 + 0.00259t - 1.32636 \times 10^{-5}t^2 + 3.33877 \times 10^{-8}t^3 - 4.0335 \times 10^{-11}t^4 + 1.89828 \times 10^{-14}t^5$$

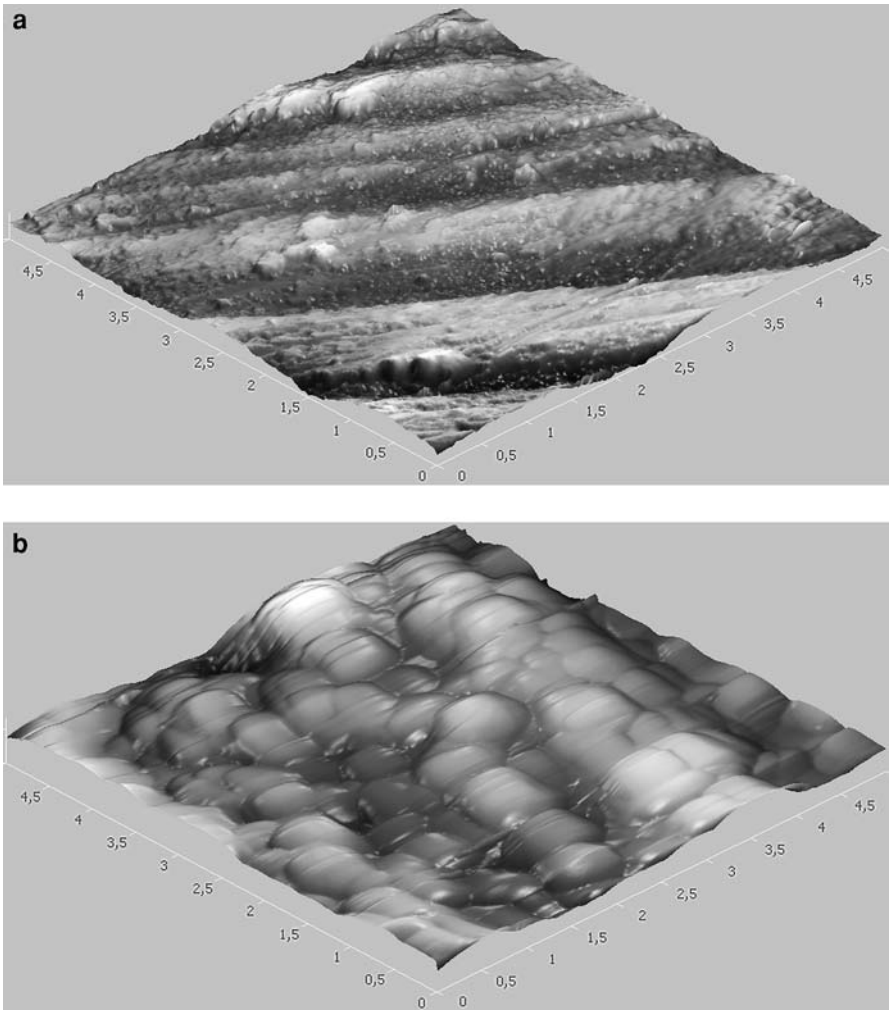

Fig. 7 AFM picture of the specimen from the AM60 alloy: before oxidation (**a**), and after oxidation (**b**), at 400 °C

$$\Delta m_{AZ91} = 99.9179 + 0.0037t - 2.13318 \times 10^{-5}\, t^2 + 6.00119 \times 10^{-8} t^3 - 7.32255 \times 10^{-11} t^4 + 3.22439 \times 10^{-14} t^5$$

$$\Delta m_{AE42} = 99.94066 + 0.00321t - 1.87755 \times 10^{-5} t^2 + 5.2823 \times 10^{-8} t^3 - 6.87294 \times 10^{-11} t^4 + 3.30968 \times 10^{-14} t^5$$

$$\Delta m_{AM60} = 100.04052 + 4.90799 \times 10^{-4} t - 3.92013 \times 10^{-7} t^2 + 6.32061 \times 10^{-10} t^3$$

At 450 °C:

$$\Delta m_{AM50} = 99.55591 + 0.00222t$$

$$\Delta m_{AE42} = 99.70671 + 7.42442 \times 10^{-4} t$$

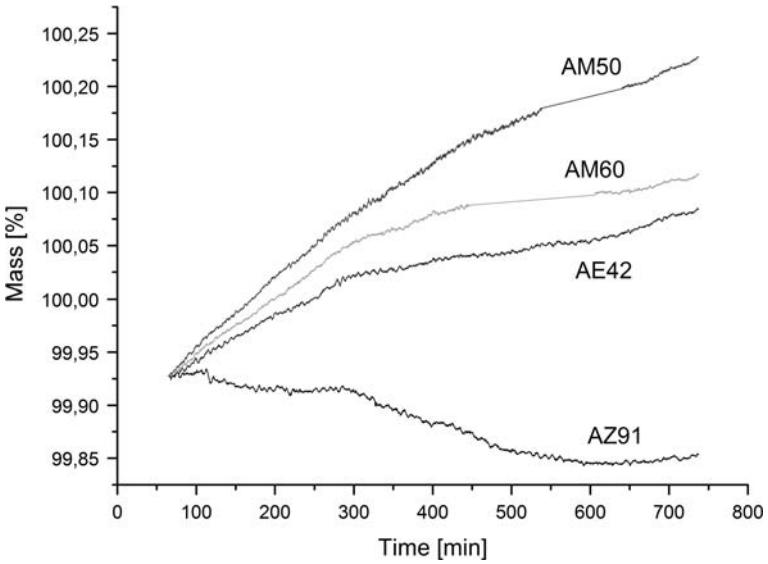

Fig. 8 Mass changes as a time function for all the specimens at 200 °C

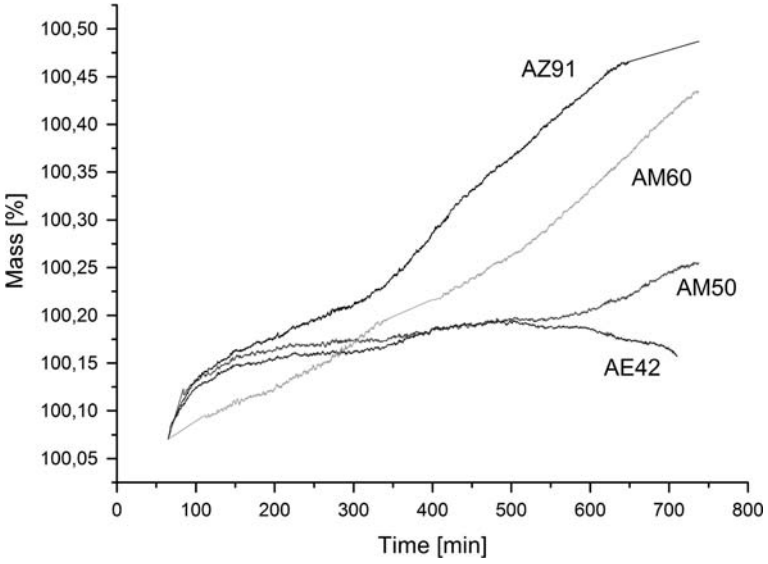

Fig. 9 Mass changes as a time function for all the specimens at 400 °C

$$\Delta m_{AM60} = 99.26979 + 0.00712t - 1.12601 \times 10^{-5}t^2 + 1.26182 \times 10^{-8}t^3$$
$$\Delta m_{AZ91} = 121.55408 - 0.74693t + 0.0083t^2 - 3.16601 \times 10^{-5}t^3 + 5.24557 \times 10^{-8}t^4 - 3.22361 \times 10^{-11}t^5$$

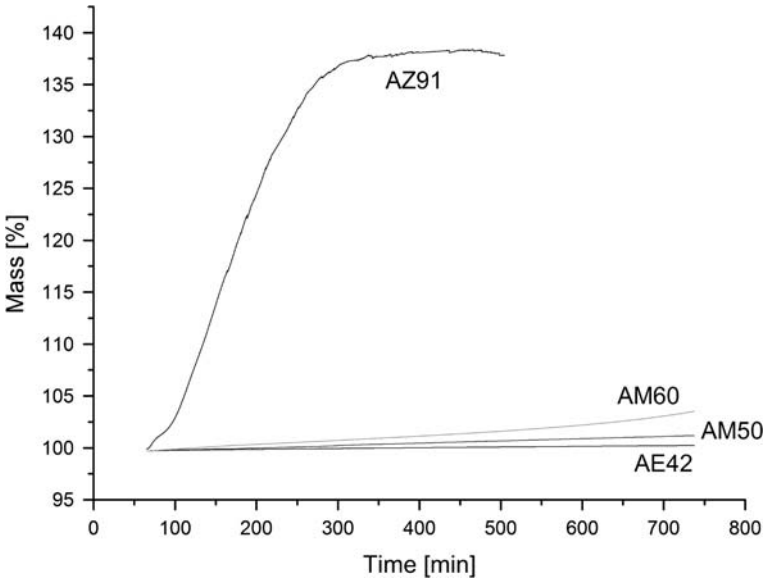

Fig. 10 Mass changes as a time function for all the specimens at 450 °C

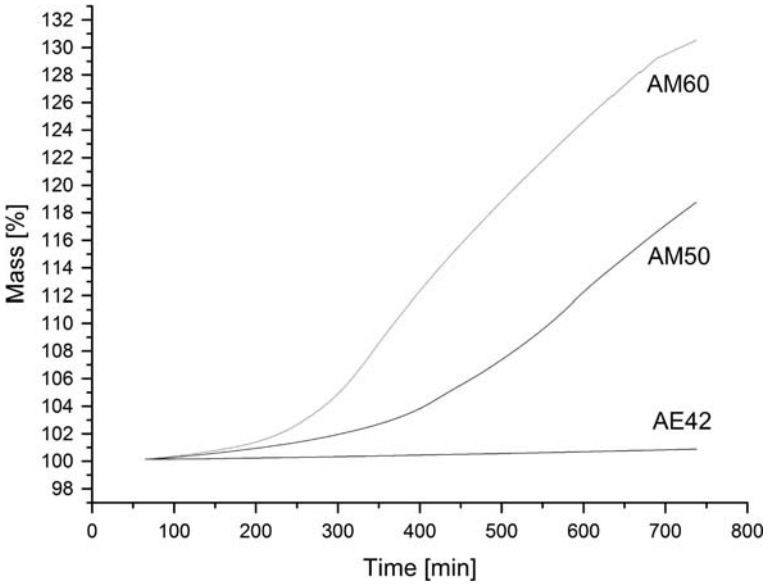

Fig. 11 Mass changes as a time function for all the specimens at 500 °C

At 475 °C:

$$\Delta m_{AM50} = 98.43285 + 0.03175t - 1.65827 \times 10^{-4}t^2 + 4.01739 \times 10^{-7}t^3 - 2.50182 \times 10^{-10}t^4$$

$$\Delta m_{AE42} = 100.01846 + 0.00112\ t$$
$$\Delta m_{AM60} = 99.75402 + 0.02563t - 3.45083 \times 10^{-4}t^2 + 1.78234 \times 10^{-6}\ t^3 - 2.80083 \times 10^{-9}t^4 + 1.43864 \times 10^{-12}t^5$$

Figures 12 and 13 present the comparison of DSC curves of the examined Mg-alloys. During the heating of Mg–Al alloys, two regions of melting were detected, except with the AE42 alloy. The first peaks on the curves in the lower temperature interval (419–431 °C) could be attributed to the melting of eutectic ($\alpha_{Mg} + Al_{17}Mg_{12}$). Because of different fractions of the eutectic, the areas under the curves, that represented the consumed heat and thus the quantity of eutectic too, differed. The second peaks on the curves indicated the melting of the α_{Mg} primary phase in all the alloys. They had different courses because of different amounts of Al in the alloys, and melting commenced the first with the alloys having higher amounts

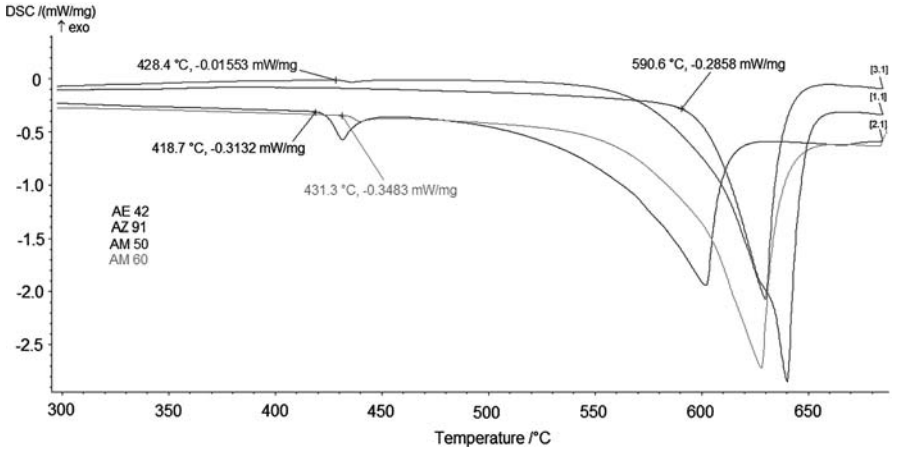

Fig. 12 DSC analyses of the melting process of Mg-alloys

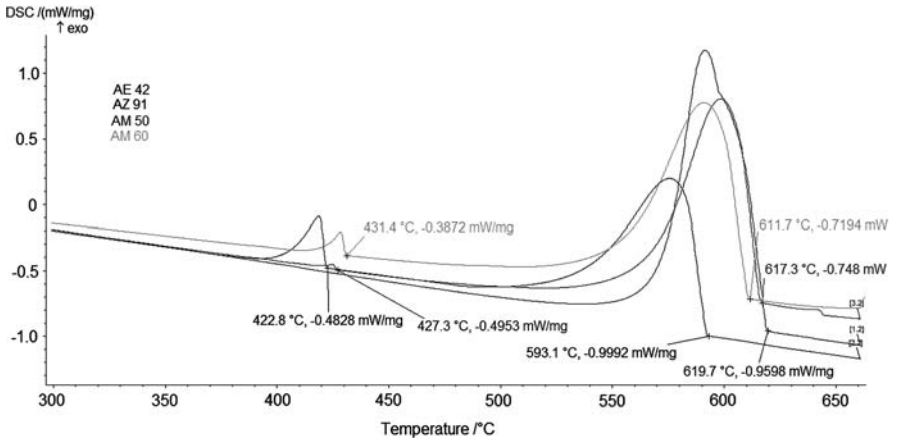

Fig. 13 DSC analyses of solidification of Mg-alloys

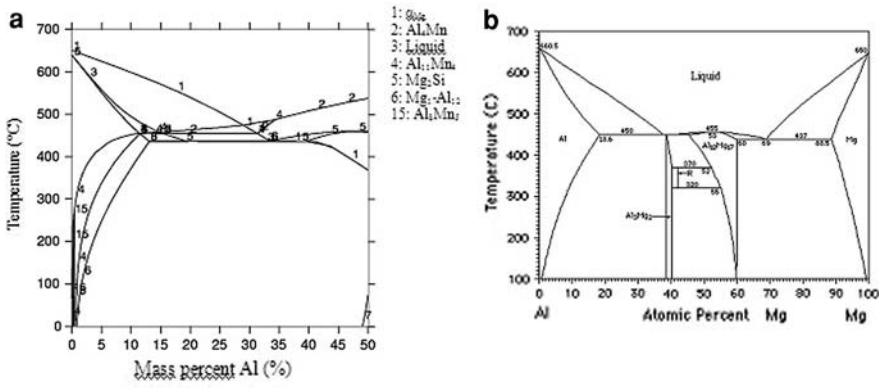

Fig. 14 Calculated phase diagram of the examined AM60 alloy (containing 0.028% Si, 0.33% Mn, and 0.05 Zn) (**a**), and the Al–Mg binary phase diagram (**b**) [5]

of aluminium. This meant that aluminium decreased the alloy melting point and it influenced the amount of the ($\alpha_{Mg} + Al_{17}Mg_{12}$) eutectic in the microstructure too. Considering the phase diagram (Fig. 14), all the alloys are in the range where eutectic should not be formed. This means that eutectic is a non-equilibrium phase.

The experiments have shown that the oxidation took place in heating and it progressed when holding specimens at constant elevated temperature. This oxide layer had a "protective" nature and grew unisotropically across the microstructure; it was stable under certain defined conditions and its thickness partly depended on the temperature and the time of oxidation.

Equilibrium melting point of the eutectic is 437 °C (Fig. 14b). The DSC determined the temperature of eutectic melting at 431 °C (Fig. 13). The simple TA of examined alloy specimens gave the eutectic temperature of 418 °C (Fig. 15). At this temperature the first liquid phase [11] appeared. The morphology of uniform oxide distribution was changed into oxide "sponges" that were formed due to the evaporation of magnesium. Oxidation became more intense with time because of long exposure to higher temperatures. Under such conditions the diffusion of the

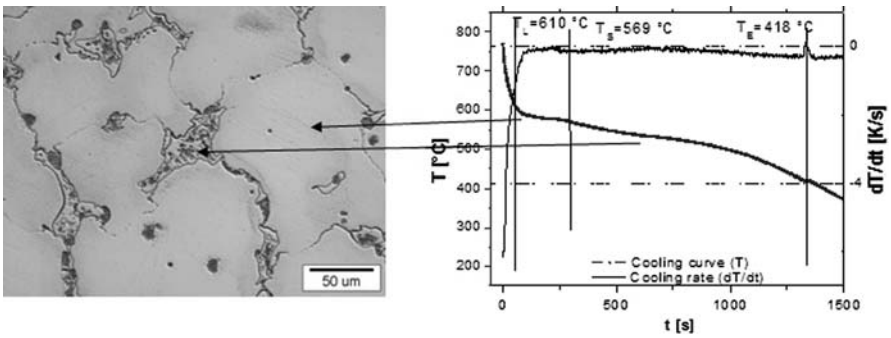

Fig. 15 Microstructure and the cooling curve of the examined AM60 alloy (containing 0.028% Si, 0.33% Mn, and 0.05 Zn) at the cooling rate of 5.7 K/s

magnesium to the surface is intense and the oxide grows in the form of the so called "sponges", until the complete material is "disintegrated".

Conclusions

The purpose of the examination was to determine the course of oxidation of the Mg alloys in the oxygen atmosphere at different temperatures. The results showed that the oxide layer could protect material against the progressive oxidation until some critical temperature has been reached. The nature of the oxide layer depended on several external conditions, such as atmosphere, temperature of the oxidation process, and also on the type of alloy. Regarding the obtained results the following conclusions can be made:

- The heating and cooling DSC curves indicated the course of melting and of solidification of Mg–Al alloys. The additions of Al decreased the liquidus temperatures. DSC curves showed that the second peak appeared on the solidification curves when alloys contained 4 or more mass% of Al. Optical microscopy revealed that this was due to non-equilibrium eutectic crystallization during the cooling process.
- TG curves indicated the course of oxidation. It has been proved that in all the examined alloys during the heating to the oxidation temperature, a thin oxide layer with a protective nature was formed. This layer was independent of the alloy composition and it was stable till the alloy melted down. The alloys that contained eutectic phase in their microstructure were protected by the oxide layer up to the first incipient fusion (equilibrium up to 437 °C). In the alloys without the eutectic phase the protective oxide layer existed to higher temperatures (at least up to 450 °C). In the alloys with eutectic phase the protective oxide layer was destroyed above the eutectic temperature and under these conditions the so-called spongy growth of oxide became evident. Oxidation of this kind is destructive and usually leads to complete degradation of the material.
- It is evident that the most stable alloy at high temperatures was the AE42 alloy and the most unstable one was the AZ91 alloy. Alloys with higher Al additions had lower corrosion stability.
- After the 12 h oxidation of the AM60 alloy it was found that the concentration of the oxygen was increasing to some depth and it remained constant afterwards. The fractions of magnesium and oxygen did not change. The concentrations of aluminium and carbon were reduced to only few at. %.
- The kinetic model of high-temperature oxidation of examined cast magnesium alloys was made regarding the time and temperature.

References

1. K. U. Kainer and F. Von Buch, in *Magnesium-Alloys and Technologies. Institut für Werkstoffforschung,* ed. V. Kainer, Trans. F. Kaiser (Wiley-VCH Verlag GmbH & Co, Weinhein, 2003), p. 1.

2. L. Vehovar, in *Korozija kovin in korozijsko preskušanje* (Ljubljana, 1991), p. 1.
3. P. Kurze, in *Magnesium-Alloys and Technologies*, ed. V. Kainer, Trans. F. Kaiser (Wiley-VCH Verlag GmbH & Co, Weinheim, 2003), p. 218.
4. E. Ghali, W. Dietzel, and K. U. Kainer, *Journal of Material Engineering and Performance* **13**, 7 (2004).
5. T. B. Massalski and H. Okamoto, in *Binary Alloys Phase Diagrams*, eds. P. R. Subramanian and L. Kaprzak, 2nd edn. (ASM, Metal Park, Ohio, 1990).
6. F. Czerwinski, *Journal of the Minerals, Metals and Materials Society* **56**, 29 (2004).
7. C. Lea and J. Molinari, *Journal of Material Science* **19**, 2336 (1984).
8. J. Medved and P. Mrvar, in *High-temperature Oxidation of Mg Alloys,* Vol. 3 (Livarski vestnik), p. 2006.
9. F. Czerwinski, *Corrosion Science* **46**, 377 (2004).
10. F. Czerwinski, *Acta Materialia* **50**, 2639 (2002).
11. J. Medved and P. Mrvar, *Materials Science Forum* **508**, 603 (2006).